Thermodynamics and heat transport in the quantum spin liquid candidates $NaYbS_2$ and $NaYbSe_2$

N. Li,[1] M. T. Xie,[2,3] Q. Huang,[4] Z. W. Zhuo,[2,3] Z. Zhang,[2] E. S. Choi,[5] Y. Y. Wang,[1] H. Liang,[1] Y. Sun,[1] D. D. Wu,[1] Q. J. Li,[6] H. D. Zhou,[4] G. Chen,[7,*] X. Zhao,[8,†] Q. M. Zhang,[2,3,‡] and X. F. Sun[1,8,9,§]

[1]*Anhui Provincial Key Laboratory of Magnetic Functional Materials and Devices, Institutes of Physical Science and Information Technology, Anhui University, Hefei, Anhui 230601, People's Republic of China*

[2]*Beijing National Laboratory for Condensed Matter Physics, Institute of Physics, Chinese Academy of Sciences, Beijing 100190, People's Republic of China*

[3]*School of Physical Science and Technology, Lanzhou University, Lanzhou 730000, People's Republic of China*

[4]*Department of Physics and Astronomy, University of Tennessee, Knoxville, Tennessee 37996, USA*

[5]*National High Magnetic Field Laboratory, Florida State University, Tallahassee, Florida 32310-3706, USA*

[6]*School of Physics and Optoelectronics, Anhui University, Hefei, Anhui 230061, People's Republic of China*

[7]*International Center for Quantum Materials, School of Physics, Peking University, Beijing 100871, China*

[8]*School of Physics Sciences, University of Science and Technology of China, Hefei, Anhui 230026, People's Republic of China*

[9]*Collaborative Innovation Center of Advanced Microstructures, Nanjing University, Nanjing, Jiangsu 210093, People's Republic of China*

(Received 21 September 2024; revised 22 November 2024; accepted 25 November 2024; published 9 December 2024)

We study the ultralow-temperature thermodynamics and thermal conductivity (κ) of the single-crystal rare-earth chalcogenides $NaYbS_2$ and $NaYbSe_2$, which have an ideal triangular lattice of the Yb^{3+} ions and have been proposed to be quantum spin liquid candidates. The magnetic specific heat divided by temperature $C_{\rm mag}/T$ is nearly constant at $T < 200$ mK, which is indeed the indication of the gapless magnetic excitations with a constant density of states. However, we observe a vanishingly small residual term κ_0/T, which points to the absence of mobile fermionic excitations in these materials. Both the weak temperature dependence of κ and the strong magnetic-field dependence of κ suggest the significant scattering between the spinons and phonons, which actually supports the existence of a gapless or tiny-gapped quantum spin liquid. Moreover, the $\kappa(B)/\kappa(0)$ isotherms show a series of field-induced magnetic transitions for $B \parallel a$, confirming the easy-plane anisotropy, which is consistent with the results of ac magnetic susceptibility. We expect our results to inspire further interests in the understanding of the spinon-phonon coupling in the spin liquid systems.

DOI: 10.1103/PhysRevB.110.224414

I. INTRODUCTION

In low-dimensional quantum magnets, the strong frustration effect originating from the competing magnetic exchange interactions suppresses conventional long-range order, together with the small spin quantum number, leading to an exotic quantum disorder state without breaking any symmetry even at 0 K—the quantum spin liquid (QSL). It was originally proposed by Anderson in 1973 based on the two-dimensional triangular lattice antiferromagnet, and then applied to explain the mechanism of high-temperature superconductivity [1–5]. Since then, many theoretical and experimental efforts have been devoted to QSL. Theoretical studies have proposed several kinds of QSLs, including a gapless $U(1)$ Dirac QSL, a gapped Z_2 QSL, and a chiral spin liquid [6,7]. Experimentally, various types of QSL candidates have been discovered in two-dimensional triangular lattice, kagome lattice, honeycomb lattice, or three-dimensional pyrochlore structures.

It is well known that spin-1/2 triangular-lattice antiferromagnets are ideal QSL candidates. $EtMe_3Sb[Pd(dmit)_2]_2$ and κ-$(BEDT\text{-}TTF)_2Cu_2(CN)_3$ are early found organic QSL candidate materials and have been widely studied [8,9]. And then, a variety of inorganic materials have emerged, including $Ba_3CuSb_2O_9$, $YbMgGaO_4$, $TbInO_3$, $NaBaCo(PO_4)_2$, $PrMAl_{11}O_{19}$ (M = Mg, Zn), $NdTa_7O_{19}$, and $ARECh_2$ (A = alkali, Re = rare earth, Ch = O, S, Se) [10–18]. Among them, rare-earth-based spin frustrated materials have attracted much attention, in which the strong spin-orbit coupling of rare-earth ions can realize an effective $J_{eff} = 1/2$ moment and strong quantum fluctuations stabilize the QSL state. In particular, a $4f$-based compound $YbMgGaO_4$ has been investigated extensively. The absence of long-range magnetic ordering down to several tens of millikelvins, a $T^{2/3}$ behavior of magnetic specific heat [11], a small residual thermal conductivity κ_0/T [$\sim$0.0058 W/(K^2 m)] [19], and a continuous magnetic excitation spectrum [20,21] are attributed to the gapless QSL ground state with spinon Fermi surface. On the contrary, the frequency dependence of the ac susceptibility and a persistent excitation continuum at polarized field [19,21] question the QSL ground state. The random distribution of Mg^{2+} and Ga^{3+} ions may play a crucial role in the controversy on the magnetic ground state of $YbMgGaO_4$ [22]. To better characterize the

*Contact author: chenxray@pku.edu.cn
†Contact author: xiazhao@ustc.edu.cn
‡Contact author: qmzhang@ruc.edu.cn
§Contact author: xfsun@ahu.edu.cn

actual physics of QSL, it is necessary to discover new QSL candidates to eliminate disorder effects.

The Yb delafossites NaYbCh_2 (Ch = O, S, Se) were found to be the promising QSL materials, in which Yb^{3+} ions form an ideal triangular lattice and free from mixing disorder. The magnetic properties of NaYbCh_2 can be systematically tuned by changing the chalcogen ions (intralayer interactions). Previous studies reported the power-law temperature dependence of the magnetic specific heat and the continuous magnetic excitations observed by inelastic neutron scattering (INS), indicative of the gapless $U(1)$ QSL with spinon Fermi surface [23–25]. The fingerprints of the gapless spinon Fermi surface are (i) a broad and continuous magnetic excitations spectrum in INS experiments [20,21,26]; (ii) a power law temperature dependence of magnetic specific heat ($C \sim T^{\alpha}$) [11,27,28]; and (iii) a finite residual thermal conductivity κ_0/T at 0 K [8,12,29–31]. Obviously, NaYbCh_2 exhibit the first two hallmarks and lack the experimental studies of low-temperature thermal conductivity due to the challenge in growing high-quality single crystals. For $NaYbO_2$, all experimental research is based on the polycrystalline samples and limits the further characterization. For $NaYbS_2$ and $NaYbSe_2$, researchers have successfully grown single-crystal samples, but they are so thin and fragile that the high-quality heat transport measurement is still very challenging. In this regard, one earlier work reported the ultralow-temperature κ results of $NaYbSe_2$ single crystals [32], which however displayed a puzzling peak at 5 T on the $\kappa(B)$ curves ($B \parallel c$) since all the existing experimental studies do not suggest any magnetic transition at this critical field.

In this work, we have grown high-quality $NaYbS_2$ and $NaYbSe_2$ single crystals and performed ultralow-temperature thermal conductivity measurement, as well as the ultralow-temperature ac magnetic susceptibility and specific heat measurements. In addition to confirming the absence of long-range magnetic order down to several tens of millikelvins and the linear temperature dependent magnetic specific heat, we observed a vanishingly small residual term κ_0/T for both materials, which indicates that there are no mobile fermionic excitations. Moreover, we observed a series of field-induced magnetic transitions for $B \parallel a$, including the 1/3 magnetization plateau associated with an up-up-down spin structure that demonstrates the easy-plane properties of $NaYbS_2$ and $NaYbSe_2$.

II. EXPERIMENTS

High-quality $NaYbS_2$ and $NaYbSe_2$ single crystals were grown by the flux method [17,33–35]. Large and shiny thin-pallet-like crystals were obtained. The important progress of our crystal growth is that the thickness of single crystals reaches several tens of micrometers, which guarantees the reliable heat transport measurements. The ac susceptibility was measured using the conventional mutual inductance technique (with a combination of ac current source and a lock-in amplifier) at the SCM1 dilution fridge magnet of the National High Magnetic Field Laboratory, Tallahassee [36]. The typical ac field strength is 1.1–1.6 Oe. The specific heat was measured by relaxation technique using a physical property measurement system (PPMS) (DynaCool, Quantum Design) with a dilution insert. The heat transport measurements were performed by using a "one heater, two thermometers" method in a ^{3}He/^{4}He dilution refrigerator (70 mK $< T <$ 1 K) and ^{3}He refrigerator (0.3 K $< T <$ 30 K), equipped with a 14 T superconducting magnet. The samples were cut into dimensions of $2.13 \times 1.56 \times 0.052$ mm^3 and $3.00 \times 1.07 \times 0.029$ mm^3 for $NaYbS_2$ and $NaYbSe_2$, respectively, with the c axis along the thickness direction. The heat currents (J) were along the longest dimensions in the a axis, and the magnetic fields were applied along either the c axis ($B \perp J$) or the a axis ($B \parallel J$).

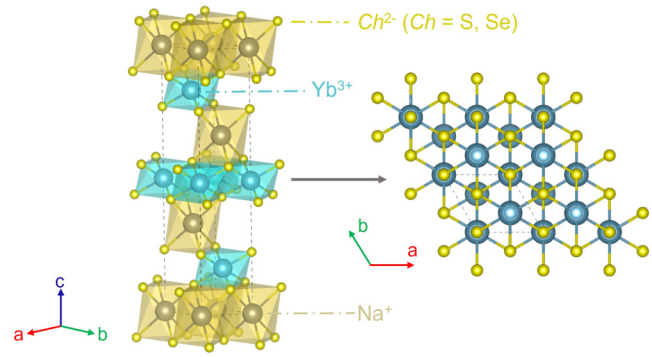

FIG. 1. Crystal structure of $NaYbS_2$ and $NaYbSe_2$ and the schematic illustration of the perfect triangular layer with the Yb^{3+} ions.

III. RESULTS AND DISCUSSION

A. Crystal structure and magnetic susceptibility

Figure 1 shows the crystal structure of $NaYbS_2$ and $NaYbSe_2$, in which the magnetic Yb^{3+} ions form ideal triangular lattice layers that are separated by the nonmagnetic NaCh_6 octahedra along the c axis. It is notable that the YbCh_6 octahedra edge-shared with NaCh_6 octahedra and are weakly distorted. The tilt of the $YbSe_6$ octahedra is smaller than that of YbS_6 octahedra, which is related to the larger radius of Se^{2-} and leads to the difference of intralayer interactions between $NaYbSe_2$ and $NaYbS_2$. Due to the large difference in ionic size between Na^+ and Yb^{3+}, the antisite disorder is much smaller than that of the Yb-based QSL candidate $YbMgGaO_4$ with Mg^{2+}/Ga^{3+} site disorder [19]. The site disorder in $NaYbS_2$ and $NaYbSe_2$ has been well studied. For $NaYbS_2$, the results of x-ray diffraction (XRD), scanning electron microscopy (SEM), electron spin resonance (ESR), and nuclear magnetic resonance (NMR) all evidenced an absence of inherent structural distortions [24,42]. For $NaYbSe_2$, the previous literatures have reported the absence of intrinsic structural disorder by using XRD, ESR, NMR, and neutron scattering measurements [37,38]. An exceptional result is that a small amount of Yb occupying the Na site was probed by using single-crystal XRD and the inductively coupled plasma measurements [25]. The structural and compositional characterizations of these single crystals have been reported in some of our previous papers [17,34,35]. However, we have not carried out deeper experimental characterization of the site disorder in the samples used in the present work.

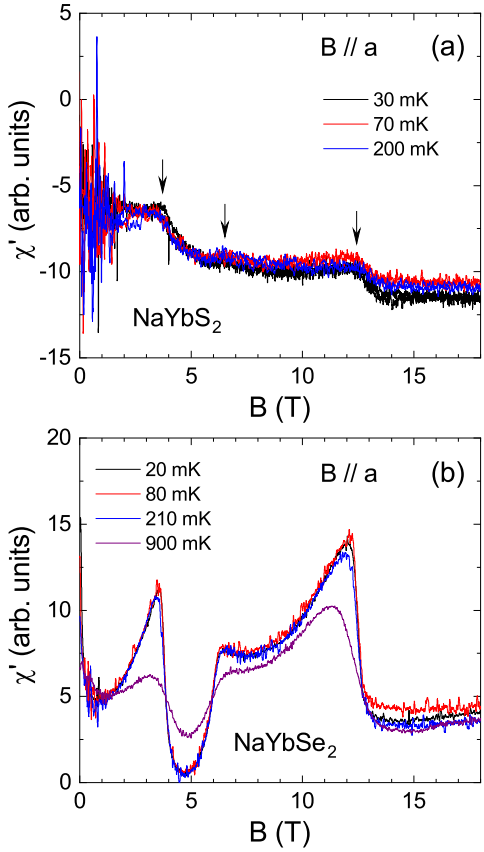

FIG. 2. Real component of the ac magnetic susceptibility as a function of dc field at different temperatures with $B \parallel a$ for $NaYbS_2$ and $NaYbSe_2$, respectively. The arrows indicate the weak peaks of $NaYbS_2$ data.

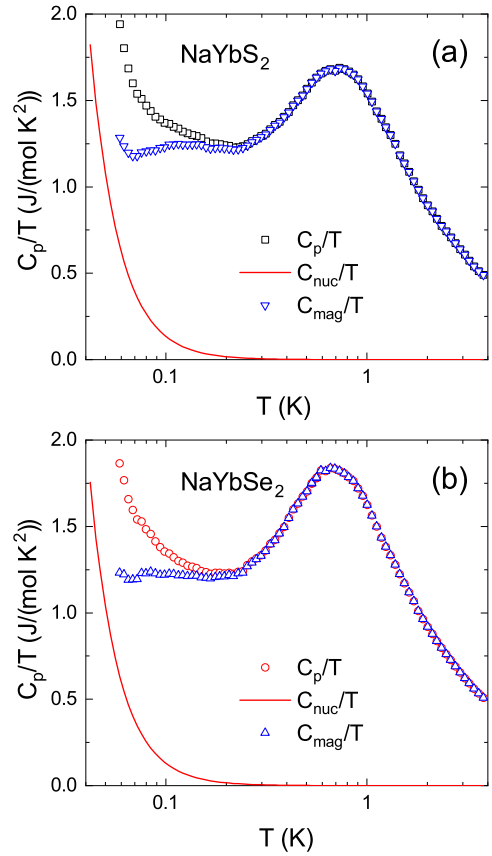

FIG. 3. Temperature dependence of the specific heat divided by temperature, C_p/T, for $NaYbS_2$ and $NaYbSe_2$ single crystals at zero magnetic field. The red lines are the estimated nuclear Schottky contributions $C_{\rm nuc}/T$. Also shown are the magnetic specific heat divided by temperatures, $C_{\rm mag}/T$.

Figure 2(a) shows the field dependence of ac susceptibility $\chi'(B)$ measured at selected temperatures with $B \parallel a$ for $NaYbS_2$. At $T = 30$ mK, the $\chi'(B)$ curve displays three weak peaks around 3.5, 6.5, and 12.5 T, respectively, and approaches saturation around 13.5 T. With increasing temperature, these peaks become weaker and broader. These transition fields are consistent with the previously reported results, indicating the magnetic transitions induced by the external magnetic field [24]. For $NaYbSe_2$, at $T = 20$ mK, the $\chi'(B)$ curve exhibits much sharper peaks around 3.5, 6.5, and 12 T with $B \parallel a$. With increasing temperature, these peaks become broader and shift to lower magnetic field, as shown in Fig. 2(b). The overall behavior of $\chi'(B)$ curves is similar to that of $NaYbS_2$. The remarkable difference is that there is a deep valley at $3.5 \sim 6.5$ T for $NaYbSe_2$, which corresponds to the $1/3M_s$ plateau (M_s is the saturation magnetization), as reported by Ranjith *et al.* [37], and indicates an up-up-down phase. This has been predicted by the mean-field theory and further confirms an easy-plane anisotropy in $NaYbSe_2$ [39]. Therefore, the present ac susceptibility data are basically consistent with the previous magnetization studies. In passing, we explain a bit about the difference of ac susceptibility data between $NaYbS_2$ and $NaYbSe_2$. The ac susceptibility measurement was performed using homemade ac coils [36]. Different coils lead to different background of ac signal. The data of $NaYbS_2$ and $NaYbSe_2$ were obtained on two different coils and the coil for $NaYbS_2$ has large background. This is the main reason for there being no very clear valley feature of $NaYbSe_2$ data.

We recently noticed a study on $NaYbSe_2$ by Scheie *et al.* that reported the ultralow-temperature ac susceptibility for not only $B \parallel a$ but also $B \parallel c$ [38]. It can be seen that our susceptibility data are consistent with theirs. It should be pointed out that their data for $B \parallel c$ show a very broad and weak peaklike feature at $\sim$7 T, which behaved significantly differently from those for $B \parallel a$.

B. Specific heat

To characterize the thermodynamics of $NaYbS_2$ and $NaYbSe_2$ single crystals, the low-temperature specific heat measurements were performed down to 60 mK with external magnetic field along the c axis. As shown in Fig. 3, the zero-field specific heat is almost identical for $NaYbS_2$ and $NaYbSe_2$, and there is no signature of long-range magnetic order. The upturn at ultralow temperatures originates from the nuclear Schottky contribution, which can be simply described by $C_{\rm nuc} \propto T^2$ [25,37]. The plot C_p/T vs T displays a broad peak between 0.2 and 1.5 K, which is a common behavior observed in some other QSL candidates, such as

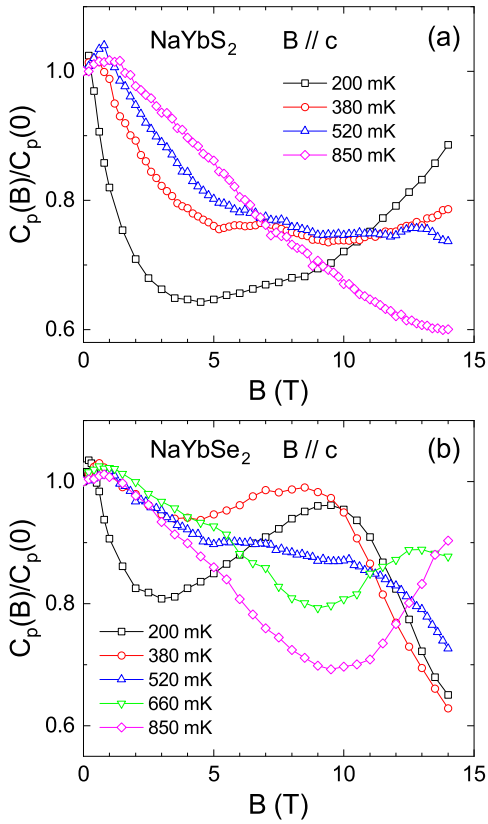

FIG. 4. Magnetic field dependence of specific heat for $NaYbS_2$ and $NaYbSe_2$ single crystals with $B \parallel c$.

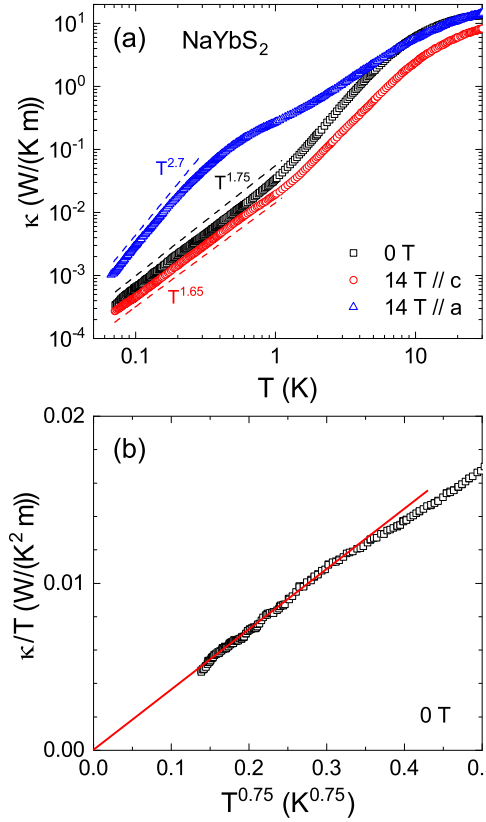

FIG. 5. (a) Temperature dependence of the thermal conductivity of $NaYbS_2$ single crystal in zero and 14 T magnetic field along the c axis or the a axis. The dash lines indicate the power law temperature dependence. (b) Zero-field thermal conductivity data plotted as κ/T vs $T^{0.75}$ at very low temperatures and the solid line shows the linear fitting. There is a negligibly small residual term ($\kappa_0/T = 0$).

$YbMgGaO_4$ and $NaYbO_2$ [11,40]. After subtracting the estimated nuclear Schottky contributions, the obtained magnetic specific heat $C_{\rm mag}$ shows a nearly linear temperature dependence at low temperatures, which indicates a gapless QSL ground state with a constant density of states. All these results are reasonably consistent with the previous reports [24,25,34]. Moreover, the constant density of states at low energies can be explained by the spinon Fermi surface in QSL. Although the linear-T specific heat and the constant density of states can be understood in terms of the random field effect in the spin glass, we think this is unlikely for our systems here. There does not exist any signature of spin freezing transition in our measurement, and thus the spin glassy features are absent. The Yb^{3+} ions in these systems provide the Kramers doublet whose degeneracy is protected by the time-reversal symmetry. Unlike the non-Kramers doublets for which the random fields can be obtained by the crystal disorders, the nonmagnetic disorders cannot generate the random fields for the Kramers doublets. Thus, we think the spinon Fermi surface state is more compatible with the low-temperature specific heat behaviors.

Figures 4(a) and 4(b) show the magnetic field dependencies of specific heat of $NaYbS_2$ and $NaYbSe_2$ at selected temperatures with external magnetic field along the c axis, respectively. There are some similarities between the data of these two materials: (i) there is a weak peak at low fields, which shifts to higher magnetic field with increasing temperature and is related to the nuclear Schottky anomaly. (ii) With increasing magnetic field, some field-induced transitions appear while the overall trend is decreasing. There are also certain differences between these two materials. At $T = 200$ mK, the $C_p(B)/C_p(0)$ of $NaYbS_2$ first decreases and then increases with increasing magnetic field, exhibiting a broad valley and a kink around 4 and 10 T, respectively. However, at $T = 200$ mK, the $C_p(B)/C_p(0)$ curve of $NaYbSe_2$ exhibits a valley and a broad peak around 3 and 9 T, respectively, and the specific heat continues to decrease at high field, which is in contrast to the case of $NaYbS_2$. In addition, for $NaYbSe_2$, the low-field valley becomes weaker and shifts to higher magnetic field with increasing temperature. It is likely that these intermediate-field behaviors are correlated with the broad and weak peaklike feature of ac susceptibility data [38]. It should be pointed out that the nuclear Schottky term can also be strongly affected by the magnetic field; in particular, at very low temperatures it can be strongly suppressed upon increasing field.

C. Thermal conductivity

Figure 5(a) shows the temperature dependence of thermal conductivity for $NaYbS_2$ single crystals in zero field and in 14 T magnetic field along the c axis or the a axis. As one can see, the zero-field $\kappa(T)$ curve exhibits a $T^{1.75}$

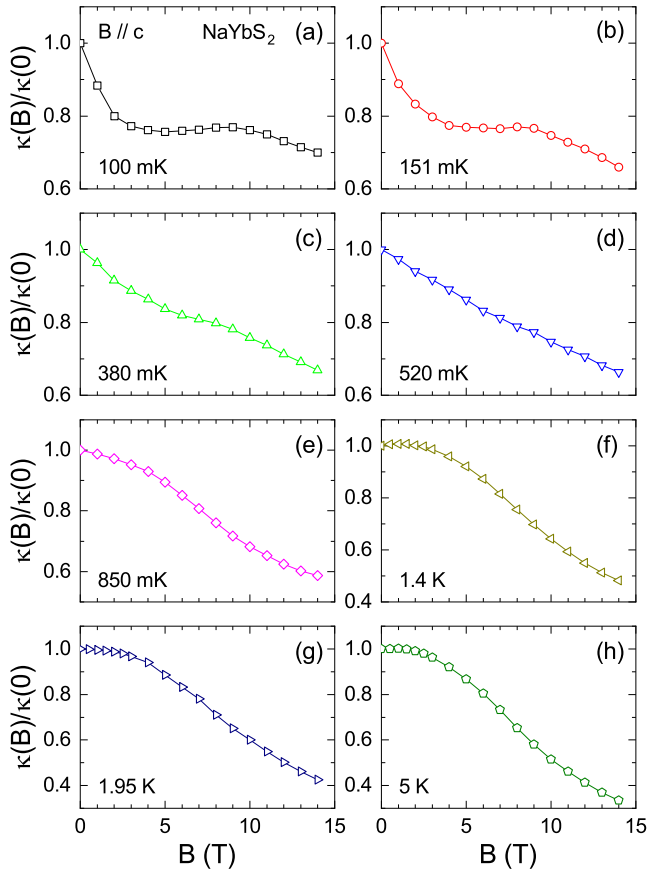

FIG. 6. Magnetic-field dependencies of thermal conductivity of $NaYbS_2$ single crystal at select temperatures for $B \parallel c$.

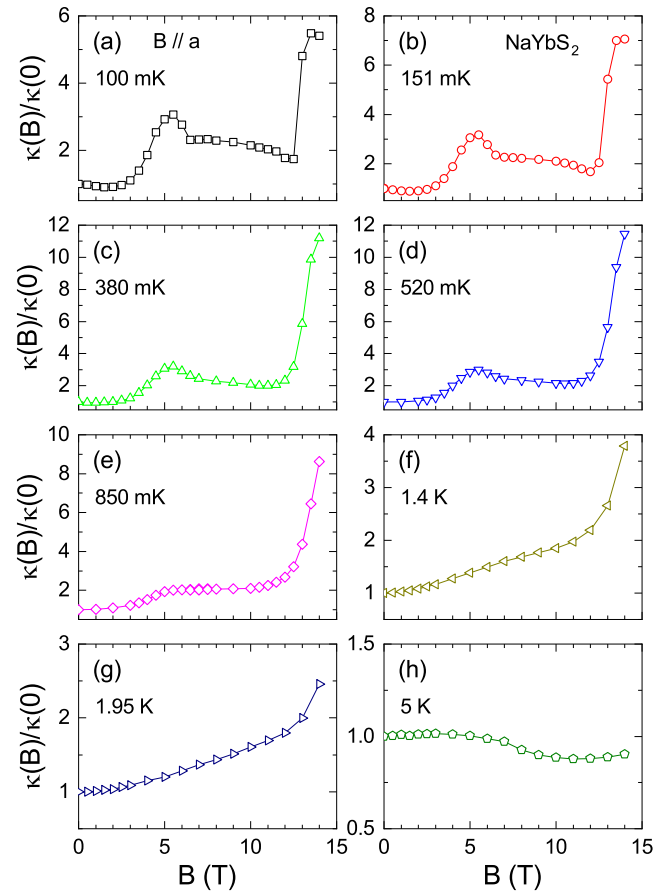

FIG. 7. Magnetic-field dependencies of thermal conductivity of $NaYbS_2$ single crystal at select temperatures for $B \parallel a$.

power law behavior at very low temperatures, which distinctly deviates from the standard phonon transport behavior (T^3 dependence) [41]. This deviation is apparently due to the strong phonon scattering by magnetic excitations. In addition, the direction of the external magnetic field has a significantly different effect on changing thermal conductivity. To be more specific, the 14 T field along the c axis slightly suppresses the thermal conductivity and the $\kappa(T)$ curve roughly obeys a $T^{1.65}$ dependence. On the contrary, the thermal conductivity is strongly enhanced for 14 T $\parallel a$ and displays a rough $T^{2.7}$ dependence at low temperatures, which is quite close to the typical behavior of phonon thermal conductivity in the boundary scattering limit. The previous studies on the magnetization of $NaYbS_2$ single crystals revealed that 14 T along the a axis can nearly fully polarize the Yb^{3+} spins, while the spin polarization field is much higher for the c direction [24,42]. Therefore, under the 14-T c-axis field the spins are still in a fluctuating state and can strongly scatter phonons, while the 14-T in-plane field can almost smear out the magnetic scattering on the phonons. Figure 5(b) shows the ultralow-temperature thermal conductivity at zero field. We fit the data by using a formula $\kappa/T = \kappa_0/T + bT^{\alpha-1}$ [8,12,19], in which the two terms represent contributions from the itinerant fermionic excitations and phonons, respectively. The fitting gives $\kappa_0/T = 0$ and $\alpha = 1.75$. The zero residual term implies the absence of the itinerant fermionic excitations in $NaYbS_2$.

Figures 6 and 7 show the $\kappa(B)$ isotherms for $NaYbS_2$ single crystals with $B \parallel c$ and $B \parallel a$, respectively. It is notable that the field dependence of κ is significantly different between the c-axis and in-plane fields. For $B \parallel c$, the κ is always suppressed by magnetic field and the suppression can reach ~40% at 14 T without saturation. At very low temperatures of 100 and 151 mK, the $\kappa(B)/\kappa(0)$ curves show a shallow and broad dip at ~5 T and an anomaly around 9 T, which disappear with increasing temperature and is consistent with the anomalies in the specific heat. In contrast, the in-plane field induces much more complex $\kappa(B)$ behavior with strong enhancement of κ at higher fields. This indicates the strong anisotropic behavior between the c-axis and in-plane fields. At very low temperatures, upon increasing field the κ first decreases slightly (~10%) and then increases nonmonotonically. The $\kappa(B)/\kappa(0)$ curves display a shallow valley around 2 T, a broad peak between 3 and 6 T, and a sharp increase around 12.5 T, accompanied with a saturation above 13.5 T. At higher temperatures, the low-field broad peak weakens and the 14-T-field enhancement can reach ~10 times without saturation. The previous magnetization and torque measurements indicated that there are four transition fields around 3.3, 6.1, 10.2, and 14.8 T for $B \parallel a$ at $T = 0.8$ K [24]. Therefore, the characteristic fields at $\kappa(B)/\kappa(0)$ isotherms are roughly consistent with these transition fields by magnetic measurements. The broad peak is related to the up-up-down phase

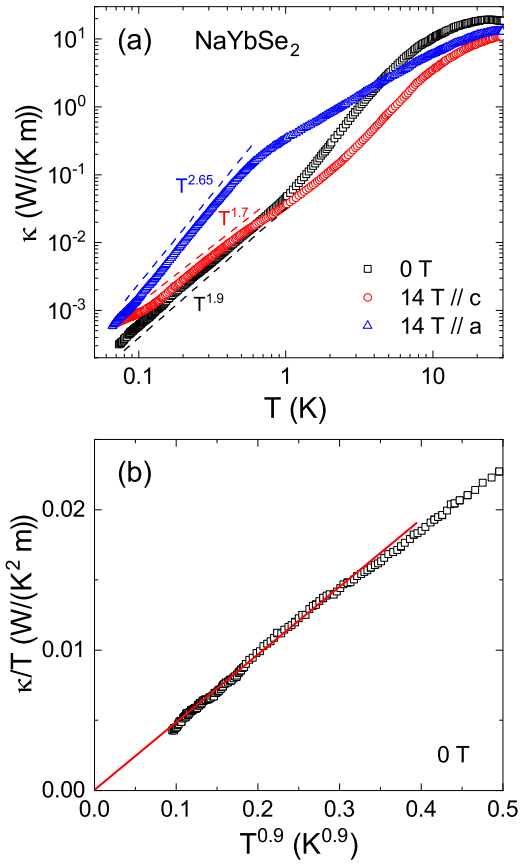

FIG. 8. (a) Temperature dependence of the thermal conductivity of $NaYbSe_2$ single crystal in zero and 14 T magnetic field along the c axis or the a axis, respectively. The dash lines indicate the power law temperature dependence. (b) Zero-field thermal conductivity plotted as κ/T vs $T^{0.9}$ at very low temperatures and the solid line shows the linear fitting. There is a negligibly small residual term ($\kappa_0/T = 0$).

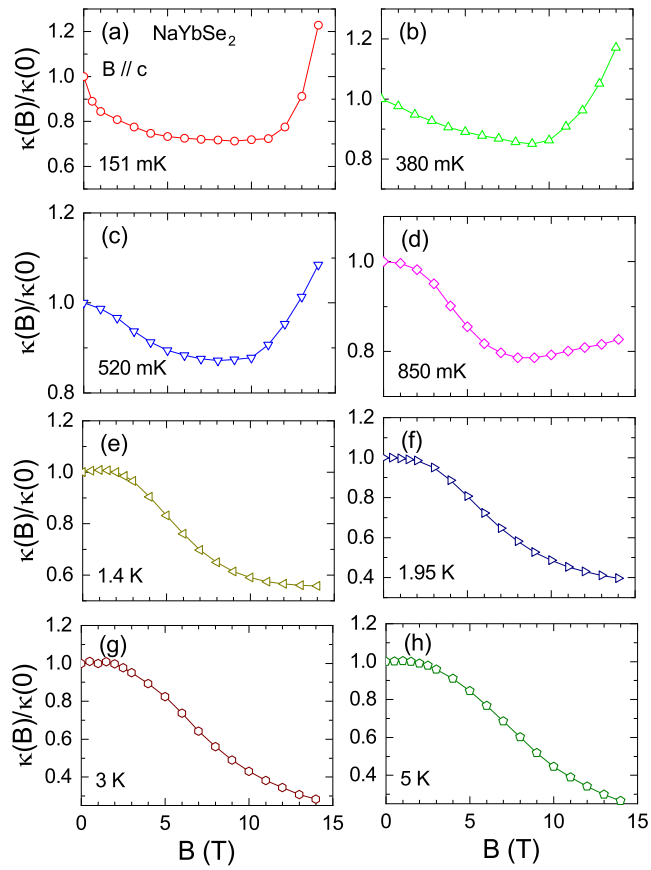

FIG. 9. Magnetic-field dependencies of thermal conductivity of $NaYbSe_2$ single crystal at select temperatures for $B \parallel c$.

and nearly disappears at $T = 850$ mK. The sharp increase of κ is associated with a phase transition from the up-up-down phase to the oblique phase. Moreover, the saturation magnetic field is reached around 13.5 T at low temperatures. At higher temperatures above 151 mK, the $\kappa(B)/\kappa(0)$ curves may saturate at fields higher than 14 T, which is consistent with higher saturation field of magnetization [24].

Figure 8(a) shows the temperature dependence of thermal conductivity for $NaYbSe_2$ single crystals in zero field and in 14 T magnetic field along the c axis or the a axis. In zero field, the $\kappa(T)$ curve exhibits a rough $T^{1.9}$ dependence, which also deviates from the standard T^3 behavior of phonon thermal conductivity at the boundary scattering limit [41] and indicates strong phonon scattering. Moreover, we observed a negligibly small κ_0/T in the κ/T vs $T^{0.9}$ plot, as shown in Fig. 8(b), which also points to the absence of mobile fermionic excitations. The different responses are observed for applying 14 T field along the c or a axis. The $\kappa(T)$ curve displays a $T^{2.65}$ dependence for 14 T field along the a axis, which is slightly weaker than the standard T^3 behavior and may be due to the specular reflections at the sample surfaces or the remaining spin-phonon scattering. For 14 T field along the c axis, the $\kappa(T)$ curve shows a $T^{1.7}$ dependence and even weaker temperature dependence below 100 mK, which also indicates the strong phonon scattering by the magnetic excitations.

The $\kappa(B)/\kappa(0)$ isotherms of $NaYbSe_2$ single crystals for $B \parallel c$ and $B \parallel a$ are shown in Figs. 9 and 10, respectively. It can be seen that the $\kappa(B)/\kappa(0)$ curves exhibit a broad valley at low fields followed by an enhancement at high fields for $B \parallel c$. The $\kappa(B)/\kappa(0)$ for $B \parallel a$ behaves very similarly to that of $NaYbS_2$, and there is a broad peak around $4 \sim 6$ T, corresponding to the up-up-down spin arrangement, which is consistent with $1/3M_s$ plateau. Moreover, a shallow dip can be observed around 12 T, which is a field-induced magnetic transition, and the $\kappa(B)$ curves finally saturate at 13 T for $T = 100$ and 151 mK. With increasing temperature, the broad peak becomes invisible and the shallow dip gradually disappears. All these critical fields are consistent with the previous magnetization results [37].

IV. DISCUSSION

It was reported that $NaYbS_2$ and $NaYbSe_2$ evidenced gapless spin excitations (spinons) from specific heat, inelastic neutron scattering (INS), and muon spin relaxation (μSR) measurements, which are connected to QSL with a spinon Fermi surface [24,25,43]. The itinerant gapless spinons are expected to contribute to the thermal conductivity, which yields a nonzero residual linear term κ_0/T at $T \to 0$ [8,12,19]. It has

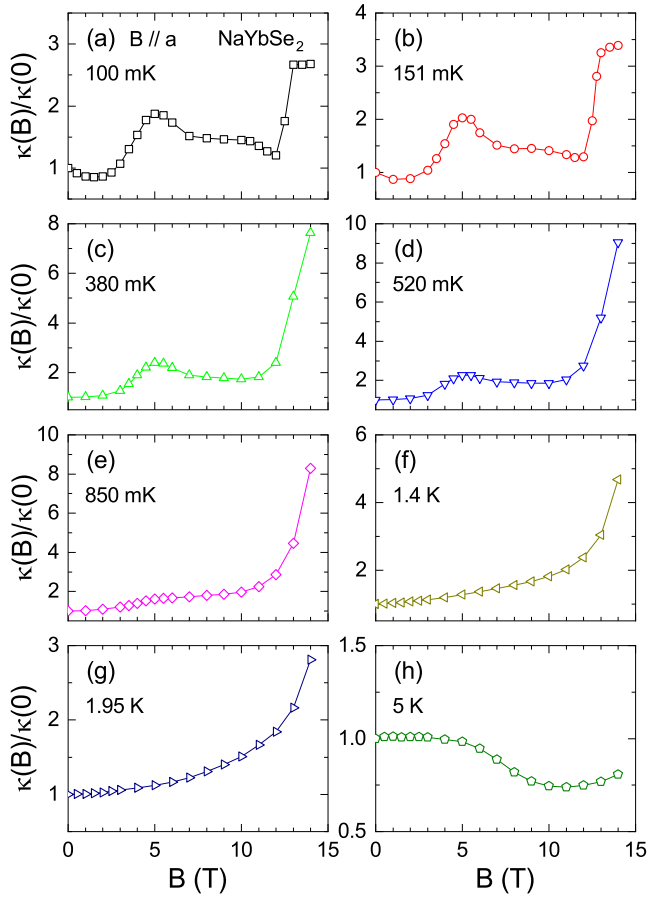

FIG. 10. Magnetic-field dependencies of thermal conductivity of $NaYbSe_2$ single crystal at select temperatures for $B \parallel a$.

become the smoking gun of the itinerant spinons and gapless QSL. However, the negligibly small κ_0/T was observed at the 0 K limit in the present work. Thus, the spinons may be strongly scattered by phonons or a minority of quasistatic spins in a fluctuating state, which was detected by μSR and NMR [32,44]. Based on the magnetic field dependence of κ, it is more likely that there are low-energy spinons scattering with phonons. It is worth pointing out that in most of the QSL candidates, there is rather strong coupling between phonons and spinons, which leads to weak temperature dependence of ultralow-temperature κ and rather small κ_0/T contributed by the spinon transport. Therefore, even though the present experiments display zero κ_0/T at zero field, the κ data actually indicate the existence of spinons that scatter with phonons. This possibility was recently found also in Ising-type QSL candidate $PrMgAl_{11}O_{19}$ [45]. It is worth pointing out that the previous ultralow-temperature κ measurement of $NaYbSe_2$ single crystals also show the absence of κ_0/T [32], although the magnetic field dependence of κ is very different from ours. Very recently, inelastic neutron scattering experiments and ac susceptibility down to 20 mK [38] suggest that there exists a very tiny gap in $NaYbSe_2$. This may offer an alternative possibility to understand our seemingly paradoxical data.

As one can see, the overall behaviors of $\chi'(B)$ curves and $\kappa(B)/\kappa(0)$ curves for $B \parallel a$ are highly similar between $NaYbS_2$ and $NaYbSe_2$, which indicates the similar in-plane properties of them with easy-plane anisotropy. However, there is a significant difference in the $\kappa(B)/\kappa(0)$ behavior with $B \parallel c$ between $NaYbS_2$ and $NaYbSe_2$. For $NaYbS_2$, the low-temperature $\kappa(B)/\kappa(0)$ curves continue to decrease as the magnetic field increases, while the low-temperature $\kappa(B)/\kappa(0)$ curves of $NaYbSe_2$ show a reduction at low field followed by an enhancement at high fields. It seems that in both materials the spin excitations (likely spinons) strongly scatter phonons rather than transport heat. High enough magnetic field along either the c axis or the a axis would suppress the spin excitations and significantly recover the phonon thermal conductivity. For $B \parallel c$, the continuous decrease of κ with field in $NaYbS_2$, which is different from the high-field increase of κ in $NaYbSe_2$, is likely due to the fact that 14 T is still far from the polarization field in $NaYbS_2$. Nevertheless, the low-field anomaly $\kappa(B)/\kappa(0)$ with $B \parallel c$ in $NaYbS_2$ may suggest some unknown field-induced transition, which is absent in $NaYbSe_2$.

V. SUMMARY

In summary, we have successfully grown high-quality single crystals of the Yb-based triangular lattice QSL candidates $NaYbS_2$ and $NaYbSe_2$, and perform the ultralow-temperature ac susceptibility, specific heat, and thermal conductivity measurements with external magnetic field along the c axis or the a axis. For $B \parallel a$, the $\chi'(B)$ and $\kappa(B)$ isotherms display similar field-induced magnetic transitions for these two materials, while the $C_p(B)$ and $\kappa(B)$ isotherms exhibit significant difference between $NaYbS_2$ and $NaYbSe_2$ for $B \parallel c$. The magnetic specific heat exhibits a nearly linear temperature dependence at $T < 200$ mK. However, the ultralow-temperature thermal conductivity shows a negligibly residual term κ_0/T. The temperature and field dependence of κ further indicate that there are spinon excitations scattering phonons rather than transporting heat in $NaYbS_2$ and $NaYbSe_2$. These results point to the gapless or tiny-gapped QSL ground state of these materials.

ACKNOWLEDGMENTS

This work was supported by the National Key Research and Development Program of China (Grants No. 2023YFA1406500 and No. 2022YFA1402704), the National Natural Science Foundation of China (Grants No. 12404043, No. 12274388, No. 12274186, No. 12174361, No. 12104010, and No. 12104011), the Nature Science Foundation of Anhui Province (Grants No. 1908085MA09 and No. 2108085QA22), the Strategic Priority Research Program of the Chinese Academy of Sciences (Grant No. XDB33010100), and the Synergetic Extreme Condition User Facility (SECUF). The work at the University of Tennessee was supported by the National Science Foundation through Award No. DMR-2003117. A portion of this work was performed at the National High Magnetic Field Laboratory, which is supported by the National Science Foundation Cooperative Agreement No. DMR-1644779 and the State of Florida.

[1] P. W. Anderson, Resonating valence bonds: A new kind of insulator? Mater. Res. Bull. **8**, 153 (1973).

[2] P. A. Lee, An end to the drought of quantum spin liquids, Science **321**, 1306 (2008).

[3] B. Normand, Frontiers in frustrated magnetism, Contemp. Phys. **50**, 533 (2009).

[4] L. Balents, Spin liquids in frustrated magnets, Nature (London) **464**, 199 (2010).

[5] C. Broholm, R. Cava, S. Kivelson, D. Nocera, M. Norman, and T. Senthil, Quantum spin liquids, Science **367**, eaay0668 (2020).

[6] Y. Zhou, K. Kanoda, and T.-K. Ng, Quantum spin liquid states, Rev. Mod. Phys. **89**, 025003 (2017).

[7] L. Savary and L. Balents, Quantum spin liquids: A review, Rep. Prog. Phys. **80**, 016502 (2017).

[8] M. Yamashita, N. Nakata, Y. Senshu, M. Nagata, H. M. Yamamoto, R. Kato, T. Shibauchi, and Y. Matsuda, Highly mobile gapless excitations in a two-dimensional candidate quantum spin liquid, Science **328**, 1246 (2010).

[9] Y. Shimizu, K. Miyagawa, K. Kanoda, M. Maesato, and G. Saito, Spin liquid state in an organic Mott insulator with a triangular lattice, Phys. Rev. Lett. **91**, 107001 (2003).

[10] H. D. Zhou, E. S. Choi, G. Li, L. Balicas, C. R. Wiebe, Y. Qiu, J. R. D. Copley, and J. S. Gardner, Spin liquid state in the $S = 1/2$ triangular lattice $Ba_3CuSb_2O_9$, Phys. Rev. Lett. **106**, 147204 (2011).

[11] Y. Li, H. Liao, Z. Zhang, S. Li, F. Jin, L. Ling, L. Zhang, Y. Zou, L. Pi, Z. Yang, J. Wang, Z. Wu, and Q. Zhang, Gapless quantum spin liquid ground state in the two-dimensional spin-1/2 triangular antiferromagnet $YbMgGaO_4$, Sci. Rep. **5**, 16419 (2015).

[12] N. Li, Q. Huang, X. Y. Yue, W. J. Chu, Q. Chen, E. S. Choi, X. Zhao, H. D. Zhou, and X. F. Sun, Possible itinerant excitations and quantum spin state transitions in the effective spin-1/2 triangular-lattice antiferromagnet $Na_2BaCo(PO_4)_2$, Nat. Commun. **11**, 4216 (2020).

[13] L. Clark, G. Sala, D. D. Maharaj, M. B. Stone, K. S. Knight, M. T. F. Telling, X. Wang, X. Xu, J. Kim, Y. Li, S.-W. Cheong, and B. D. Gaulin, Two-dimensional spin liquid behaviour in the triangular-honeycomb antiferromagnet $TbInO_3$, Nat. Phys. **15**, 262 (2019).

[14] M. Ashtar, Y. X. Gao, C. L. Wang, Y. Qiu, W. Tong, Y. M. Zou, X. W. Zhang, M. A. Marwat, S. L. Yuan, and Z. M. Tian, Synthesis, structure and magnetic properties of rare-earth $REMgAl_{11}O_{19}$ (RE = Pr, Nd) compounds with two-dimensional triangular lattice, J. Alloys Compd. **802**, 146 (2019).

[15] M. Ashtar, M. A. Marwat, Y. X. Gao, Z. T. Zhang, L. Pi, S. L. Yuan, and Z. M. Tian, $REZnAl_{11}O_{19}$ (RE = Pr, Nd, Sm–Tb): A new family of ideal 2D triangular lattice frustrated magnets, J. Mater. Chem. C **7**, 10073 (2019).

[16] T. Arh, B. Sana, M. Pregelj, P. Khuntia, Z. Jagličić, M. D. Le, P. K. Biswas, P. Manuel, L. Mangin-Thro, A. Ozarowski, and A. Zorko, The Ising triangular-lattice antiferromagnet neodymium heptatantalate as a quantum spin liquid candidate, Nat. Mater. **21**, 416 (2022).

[17] W. Liu, Z. Zhang, J. Ji, Y. Liu, J. Li, X. Wang, H. Lei, G. Chen, and Q. Zhang, Rare-earth chalcogenides: A large family of triangular lattice spin liquid candidates, Chin. Phys. Lett. **35**, 117501 (2018).

[18] J. Xing, L. D. Sanjeewa, J. Kim, G. R. Stewart, A. Podlesnyak, and A. S. Sefat, Field-induced magnetic transition and spin fluctuations in the quantum spin-liquid candidate $CsYbSe_2$, Phys. Rev. B **100**, 220407(R) (2019).

[19] X. Rao, G. Hussain, Q. Huang, W. J. Chu, N. Li, X. Zhao, Z. Dun, E. S. Choi, T. Asaba, L. Chen, L. Li, X. Y. Yue, N. N. Wang, J.-G. Cheng, Y. H. Gao, Y. Shen, J. Zhao, G. Chen, H. D. Zhou, and X. F. Sun, Survival of itinerant excitations and quantum spin state transitions in $YbMgGaO_4$ with chemical disorder, Nat. Commun. **12**, 4949 (2021).

[20] Y. Shen, Y.-D. Li, H. Wo, Y. Li, S. Shen, B. Pan, Q. Wang, H. C. Walker, P. Steffens, M. Boehm, Y. Hao, D. L. Quintero-Castro, L. W. Harriger, M. D. Frontzek, L. Hao, S. Meng, Q. Zhang, G. Chen, and J. Zhao, Evidence for a spinon Fermi surface in a triangular-lattice quantum-spin-liquid candidate, Nature (London) **540**, 559 (2016).

[21] J. A. M. Paddison, M. Daum, Z. Dun, G. Ehlers, Y. Liu, M. B. Stone, H. Zhou, and M. Mourigal, Continuous excitations of the triangular-lattice quantum spin liquid $YbMgGaO_4$, Nat. Phys. **13**, 117 (2017).

[22] Z. Zhu, P. A. Maksimov, S. R. White, and A. L. Chernyshev, Disorder-induced mimicry of a spin liquid in $YbMgGaO_4$, Phys. Rev. Lett. **119**, 157201 (2017).

[23] L. Ding, P. Manuel, S. Bachus, F. Grußler, P. Gegenwart, J. Singleton, R. D. Johnson, H. C. Walker, D. T. Adroja, A. D. Hillier, and A. A. Tsirlin, Gapless spin-liquid state in the structurally disorder-free triangular antiferromagnet $NaYbO_2$, Phys. Rev. B **100**, 144432 (2019).

[24] J. Wu, J. Li, Z. Zhang, C. Liu, Y. H. Gao, E. Feng, G. Deng, Q. Ren, Z. Wang, R. Chen, J. Embs, F. Zhu, Q. Huang, Z. Xiang, L. Chen, Y. Wu, E. S. Choi, Z. Qu, L. Li, J. Wang, H. Zhou, Y. Su, X. Wang, G. Chen, Q. Zhang, and J. Ma, Magnetic field effects on the quantum spin liquid behaviors of $NaYbS_2$, Quantum Front. **1**, 13 (2022).

[25] P.-L. Dai, G. Zhang, Y. Xie, C. Duan, Y. Gao, Z. Zhu, E. Feng, Z. Tao, C.-L. Huang, H. Cao, A. Podlesnyak, G. E. Granroth, M. S. Everett, J. C. Neuefeind, D. Voneshen, S. Wang, G. Tan, E. Morosan, X. Wang, H.-Q. Lin, L. Shu, G. Chen, Y. Guo, X. Lu, and P. Dai, Spinon Fermi Surface Spin Liquid in a Triangular Lattice Antiferromagnet $NaYbSe_2$, Phys. Rev. X **11**, 021044 (2021).

[26] T.-H. Han, J. S. Helton, S. Chu, D. G. Nocera, J. A. Rodriguez-Rivera, C. Broholm, and Y. S. Lee, Fractionalized excitations in the spin-liquid state of a kagome-lattice antiferromagnet, Nature (London) **492**, 406 (2012).

[27] S. Yamashita, Y. Nakazawa, M. Oguni, Y. Oshima, H. Nojiri, Y. Shimizu, K. Miyagawa, and K. Kanoda, Thermodynamic properties of a spin-1/2 spin-liquid state in a κ-type organic salt, Nat. Phys. **4**, 459 (2008).

[28] S. Yamashita, T. Yamamoto, Y. Nakazawa, M. Tamura, and R. Kato, Gapless spin liquid of an organic triangular compound evidenced by thermodynamic measurements, Nat. Commun. **2**, 275 (2011).

[29] C. P. Nave and P. A. Lee, Transport properties of a spinon Fermi surface coupled to a U(1) gauge field, Phys. Rev. B **76**, 235124 (2007).

[30] Y. Werman, S. Chatterjee, S. C. Morampudi, and E. Berg, Signatures of fractionalization in spin liquids from interlayer thermal transport, Phys. Rev. X **8**, 031064 (2018).

[31] H. Murayama, Y. Sato, T. Taniguchi, R. Kurihara, X. Z. Xing, W. Huang, S. Kasahara, Y. Kasahara, I. Kimchi, M. Yoshida, Y. Iwasa, Y. Mizukami, T. Shibauchi, M. Konczykowski, and Y. Matsuda, Effect of quenched disorder on the quantum spin liquid state of the triangular-lattice antiferromagnet $1T$-TaS_2, Phys. Rev. Res. **2**, 013099 (2020).

[32] Z. Zhu, B. Pan, L. Nie, J. Ni, Y. Yang, C. Chen, C Jiang, Y. Huang, E. Cheng, Y. Yu, J. Miao, A. D. Hillier, X. Chen, T. Wu, Y. Zhou, S. Li, and L. Shu, Fluctuating magnetic droplets immersed in a sea of quantum spin liquid, The Innovation **4**, 100459 (2023).

[33] Z. Zhang, X. Ma, J. Li, G. Wang, D. T. Adroja, T. P. Perring, W. Liu, F. Jin, J. Ji, Y. Wang, Y. Kamiya, X. Wang, J. Ma, and Q. Zhang, Crystalline electric field excitations in the quantum spin liquid candidate $NaYbSe_2$, Phys. Rev. B **103**, 035144 (2021).

[34] Z. Zhang, J. Li, W. Liu, Z. Zhang, J. Ji, F. Jin, R. Chen, J. Wang, X. Wang, J. Ma, and Q. Zhang, Effective magnetic Hamiltonian at finite temperatures for rare-earth chalcogenides, Phys. Rev. B **103**, 184419 (2021).

[35] W. Zhuo, Z. Zhang, M. Xie, A. Zhang, J. Ji, F. Jin, and Q. Zhang, Magnetism of $NaYbS_2$: From finite temperatures to ground state, Sci. China Phys. Mech. Astron. **67**, 107411 (2024).

[36] Z. L. Dun, M. Lee, E. S. Choi, A. M. Hallas, C. R. Wiebe, J. S. Gardner, E. Arrighi, R. S. Freitas, A. M. Arevalo-Lopez, J. P. Attfield, H. D. Zhou, and J. G. Cheng, Chemical pressure effects on magnetism in the quantum spin liquid candidates $Yb_2X_2O_7$ (X = Sn, Ti, Ge), Phys. Rev. B **89**, 064401 (2014).

[37] K. M. Ranjith, S. Luther, T. Reimann, B. Schmidt, Ph. Schlender, J. Sichelschmidt, H. Yasuoka, A. M. Strydom, Y. Skourski, J. Wosnitza, H. Kühne, Th. Doert, and M. Baenitz, Anisotropic field-induced ordering in the triangular-lattice quantum spin liquid $NaYbSe_2$, Phys. Rev. B **100**, 224417 (2019).

[38] A. O. Scheie, M. Lee, K. Wang, P. Laurell, E. S. Choi, D. Pajerowski, Q. Zhang, J. Ma, H. D. Zhou, S. Lee, S. M. Thomas, M. O. Ajeesh, P. F. S. Rosa, A. Chen, V. S. Zapf, M. Heyl, C. D. Batista, E. Dagotto, J. E. Moore, and D. A. Tennant, Spectrum and low-energy gap in triangular quantum spin liquid $NaYbSe_2$, arXiv:2406.17773.

[39] A. V. Chubukov and D. I. Golosov, Quantum theory of an antiferromagnet on a triangular lattice in a magnetic field, J. Phys.: Condens. Matter **3**, 69 (1991).

[40] M. M. Bordelon, E. Kenney, C. Liu, T. Hogan, L. Posthuma, M. Kavand, Y. Lyu, M. Sherwin, N. P. Butch, C. Brown, M. J. Graf, L. Balents, and S. D. Wilson, Field-tunable quantum disordered ground state in the triangular-lattice antiferromagnet $NaYbO_2$, Nat. Phys. **15**, 1058 (2019).

[41] R. Berman, *Thermal Conduction in Solids* (Oxford University Press, Oxford, 1976).

[42] M. Baenitz, Ph. Schlender, J. Sichelschmidt, Y. A. Onykiienko, Z. Zangeneh, K. M. Ranjith, R. Sarkar, L. Hozoi, H. C. Walker, J.-C. Orain, H. Yasuoka, J. van den Brink, H. H. Klauss, D. S. Inosov, and Th. Doert, $NaYbS_2$: A planar spin-1/2 triangular-lattice magnet and putative spin liquid, Phys. Rev. B **98**, 220409(R) (2018).

[43] Z. Zhang, J. Li, M. Xie, W. Zhuo, D. T. Adroja, P. J. Baker, T. G. Perring, A. Zhang, F. Jin, J. Ji, X. Wang, J. Ma, and Q. Zhang, Low-energy spin dynamics of the quantum spin liquid candidate $NaYbSe_2$, Phys. Rev. B **106**, 085115 (2022).

[44] R. Sarkar, Ph. Schlender, V. Grinenko, E. Haeussler, P. J. Baker, Th. Doert, and H.-H. Klauss, Quantum spin liquid ground state in the disorder free triangular lattice $NaYbS_2$, Phys. Rev. B **100**, 241116(R) (2019).

[45] N. Li, A. Rutherford, Y. Y. Wang, H. Liang, Q. J. Li, Z. J. Zhang, H. Wang, W. Xie, H. D. Zhou, and X. F. Sun, Ising-type quantum spin liquid state in $PrMgAl_{11}O_{19}$, Phys. Rev. B **110**, 134401 (2024).